Molecular-orbital Studies on Carbametallaboranes. Part 1. Icosahedral Carbaplatinaborane Polyhedra

By D. Michael P. Mingos, Department of Chemistry, Queen Mary College, Mile End Road, London E1 4NS†

Extended-Hückel molecular-orbital calculations are reported for the icosahedral platinaboranes and carbaboranes $[B_{11}\{Pt(PH_3)_2\}H_{11}]^{2-}$, $[B_{10}C\{Pt(PH_3)_2\}H_{11}]^{-}$, and $B_9C_2[Pt(PH_3)_2]H_{11}$. The failure of the polyhedral skeletal electron-counting rules when applied to carbaplatinaboranes is discussed, and attributed to the unequal bonding capabilities of the platinum $5d_{xz}$ and $5d_{yz}$ orbitals in the $Pt(PH_3)_2$ fragment. The conformations of icosahedral carbaplatinaboranes are rationalised on the basis of the symmetry characteristics of the lowest-unoccupied orbital of the carbaborane and the highest-occupied orbital of the metal-phosphine moiety. Analogous d^8 metal compounds are predicted to be stable and expected to have conformations which are complementary to those observed for d^{10} metal compounds.

In recent years the synthesis of a wide range of polyhedral carbametallaboranes, primarily by Hawthorne,[1] Grimes,[2] and their co-workers, has added a new and exciting dimension to organometallic chemistry. The development of new synthetic routes to these complex compounds has been accompanied by the development of a set of simple rules which can be reliably used to predict and rationalise the polyhedral geometries adopted by these molecules. These rules originated from a perceptive analogy [3] between clusters of transition metals and borane anions. The theoretical basis and applications of these rules have been widely reviewed [4-8] and will be touched on only briefly in this introduction. The analogy between boranes and metal clusters, it has been suggested, originates in the similar overlap integrals for the *s* and *p* valence orbitals of these elements at typical cluster bond lengths,[9] and the fact that B–H, C–H, $M(CO)_3$, and $M(\eta\text{-}C_5H_5)$ fragments are isolobal.[10,11,‡]

Recently Stone and his co-workers [12-18] showed that nucleophilic zerovalent derivatives of nickel, palladium, and platinum insert directly into *closo*-carbaborane polyhedra to form carbametallaboranes according to equation (1). Typically, two ligands, *e.g.* PR_3 or RNC,

$$\begin{array}{ll} M^0 + B_nC_2H_{n+2} \longrightarrow & B_nC_2M^{II}H_{n+2} \\ \text{polyhedron with} & \text{polyhedron with} \\ (2+n) \text{ vertices} & (3+n) \text{ vertices} \end{array} \quad (1)$$

are co-ordinated to the metal atom M, and the simple electron-counting rules mentioned above predict *closo* structures for the $B_nC_2MH_{n+2}$ polyhedra. This arises because an angular ML_2 d^{10} fragment is thought to contribute three orbitals and two electrons for skeletal bond formation.[7] However, *X*-ray crystallographic studies by Welch and his co-workers [13-18] demonstrated that such a simple interpretation is not valid. These polyhedra show a wide variation in M–C bond lengths and a simple classification of their structures as either *nido* or *closo* is not possible. In order to provide a more detailed understanding of the bonding in these interesting molecules I have completed molecular-orbital (m.o.) calculations on some model platinaboranes and carbaboranes which are based on the icosahedron. I was also intrigued by the observation that in the two isoelectronic carbametallaboranes (1) and (2) the ML_2 moiety takes up a different conformation with respect to the icosahedral fragment and have sought to explain this difference in terms of current chemical theory.

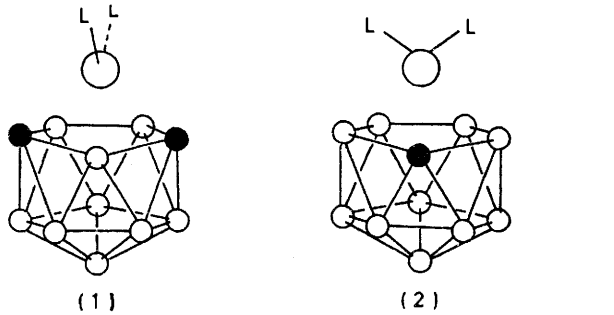

(1) (2)

e.g. $B_9(CMe^{2,4})_2[Pt(PMe_2Ph)_2^{1}]H_9$ (ref. 14)

e.g. $B_{10}[C(NMe_3)^2][Pd(CNBu^t)_2^{1}]H_{10}$ (ref. 15)

CALCULATIONS

All the calculations were made using the extended-Hückel method.[19,20] The basis set for the platinum atom consisted of 5*d*, 6*s*, and 6*p* orbitals. The *s* and *p* orbitals were described by single Slater-type wavefunctions and the *d*-orbital wave functions were taken as contracted linear combinations of two Slater-type wavefunctions. The orbital exponents were those suggested by Basch and Gray.[21] The

† *Present address:* Inorganic Chemistry Laboratory, South Parks Road, Oxford OX1 3QR.

‡ Isolobal implies that the symmetry properties and extent in space and energies of the frontier orbitals of the fragments are similar. Such fragments therefore present orbitals of like symmetry for polyhedral skeletal bond formation.

[1] M. F. Hawthorne, *J. Organometallic Chem.*, 1975, **100**, 97.
[2] D. C. Beer, V. R. Miller, L. G. Sneddon, R. N. Grimes, M. Mathau, and G. J. Pelanik, *J. Amer. Chem. Soc.*, 1973, **95**, 3046.
[3] K. Wade, *Chem. Comm.*, 1971, 792.
[4] K. Wade, *Adv. Inorg. Chem. Radiochem.*, 1976, **18**, 1.
[5] K. Wade, *Chem. in Britain*, 1975, 177.
[6] R. Mason and D. M. P. Mingos, *M.T.P. Internat. Rev. Sci., Phys. Sci. Ser. II*, 1975, **11**, 121.
[7] D. M. P. Mingos, *Nature Phys. Sci.*, 1972, **236**, 99.
[8] D. M. P. Mingos, *Adv. Organometallic Chem.*, in the press.
[9] D. M. P. Mingos, *J.C.S. Dalton*, 1974, 133.
[10] M. Elian and R. Hoffmann, *Inorg. Chem.*, 1975, **14**, 1058.
[11] M. Elian, M. M. L. Chen, D. M. P. Mingos, and R. Hoffmann, *Inorg. Chem.*, 1976, **15**, 1148.
[12] F. G. A. Stone, *J. Organometallic Chem.*, 1975, **100**, 257.
[13] M. Green, J. L. Spencer, F. G. A. Stone, and A. J. Welch, *J.C.S. Dalton*, 1975, 179.
[14] A. J. Welch, *J.C.S. Dalton*, 1975, 1473.
[15] W. E. Carroll, M. Green, F. G. A. Stone, and A. J. Welch, *J.C.S. Dalton*, 1975, 2265.
[16] A. J. Welch, *J.C.S. Dalton*, 1975, 2270.
[17] M. Green, J. A. K. Howard, J. L. Spencer, and F. G. A. Stone, *J.C.S. Dalton*, 1975, 2274.
[18] A. J. Welch, *J.C.S. Dalton*, 1976, 225.
[19] R. Hoffmann, *J. Chem. Phys.*, 1963, **39**, 1397.
[20] R. Hoffmann and W. N. Lipscomb, *J. Chem. Phys.*, 1962, **36**, 3179; **37**, 2872.
[21] H. Basch and H. B. Gray, *Theor. Chim. Acta*, 1966, **4**, 367.

parameters for the extended-Hückel calculations are summarised below: [20-22]

Orbital	Slater exponent	H_{ii}/eV	Ref.
H 1*s*	1.30	−13.60	20
B 2*s*	1.30	−15.20	20
2*p*	1.30	−8.50	20
P 3*s*	1.60	−18.60	20
3*p*	1.60	−14.00	20
Pt 6*s*	2.554	−9.80	22
6*p*	2.554	−5.35	22

Pt *d* wavefunctions:

Orbital	H_{ii}	ζ_1	C_1	ζ_2	C_2	Ref.
Pt 5*d*	−10.61	6.013	0.633	2.696	0.551	21, 22

1 eV = 96.5 kJ mol^{-1}.

The calculations were made on the ICL 1900 computer at this College using the ICON 8 programs developed by Hoffmann and his co-workers at Cornell University.[19,20]

Calculations were made on the model icosahedral clusters $[B_{11}\{Pt(PH_3)_2\}H_{11}]^{2-}$, $[B_{10}C\{Pt(PH_3)_2\}H_{11}]^-$ [see (2) above], and $B_9C_2[Pt(PH_3)_2]H_{11}$ [see (1) above]. The borane and carbaborane fragments were idealised as a *nido*, C_{5v}, icosahedral fragment with dimensions B–B = B–C = 1.750 Å. The B–H or C–H bonds were set to point towards the origin of the polyhedron and were assigned a length of 1.200 Å. The platinum atom which completes the distorted icosahedral polyhedron [see (1) and (2) above] was set to lie along the five-fold rotation axis and with Pt–C = Pt–B = 2.25 Å.[14] The geometries of the phosphine ligands were idealised and the parameters P–H = 1.42 Å and Pt–P–H = 109.4712° were used. The platinum-phosphine moiety was constrained to have C_{2v} symmetry with a P–Pt–P bond angle of 100° and Pt–P = 2.30 Å.

RESULTS AND DISCUSSION

In analysing the bonding in carbametallaboranes, such as (1) and (2), the problem has been divided into the following components: (*a*) an evaluation of the bonding capabilities of the $Pt(PH_3)_2$ fragment; (*b*) an analysis of the frontier orbitals of the *nido*-icosahedral fragment; and (*c*) the interactions between the metal and icosahedral fragments. This is not the only way of analysing the problem, but it does provide a convenient distinction between the metallic and non-metallic components of the compound.

(*a*) *The Angular* $Pt(PH_3)_2$ *Fragment.*—The angular ML_2 fragment (M = Ni, Pd, or Pt; L = PR_3 or RNC) is a common component of Group 8 organometallic chemistry and is found not only in zerovalent metal complexes such as $[Pt(olefin)(PR_3)_2]$ but also in *cis*-platinum-(II) and -(IV) complexes, *e.g. cis*-$[PtCl_2(PR_3)_2]$ and *cis*-$[PtCl_4(PR_3)_2]$.[23,24] A detailed analysis of the bonding capabilities of this fragment has not previously been given, although Burdett has discussed the *d*-orbital splitting in the related $M(CO)_2$ species.[25]

Figure 1 illustrates the computed energy levels for the C_{2v} $Pt(PH_3)_2$ fragment with a P–Pt–P bond angle of 100°. The symmetric and antisymmetric metal–phosphorus bonding molecular orbitals $1A_1$ and $1B_1$ are concentrated mainly on the phosphorus atoms but have significant metal 6*s*, $6p_x$, and $5d_{xz}$ components. The platinum 5*d* manifold of energy levels shows a particularly simple splitting pattern of four stable orbitals with more than 95% metal *d*-orbital character, *i.e. xy*, z^2, *yz*, and $x^2 - y^2$,* and a higher-lying level hybrid (*xz*) which has predominantly *xz* character (80%) but with some metal *x* character mixed in (13%). The sign of *d*–*p* mixing is such that it effectively rehybridises the *xz* orbital away from the ligands as shown in Figure 1. This orbital is the highest-occupied orbital of the fragment (h.o.m.o.) and plays an important role in determining the stereochemistries of platinum complexes. This rehybridisation phenomenon is normally associated with valence-bond theory but may also be derived from m.o. theory by using second-order perturbation-theory arguments.[10]

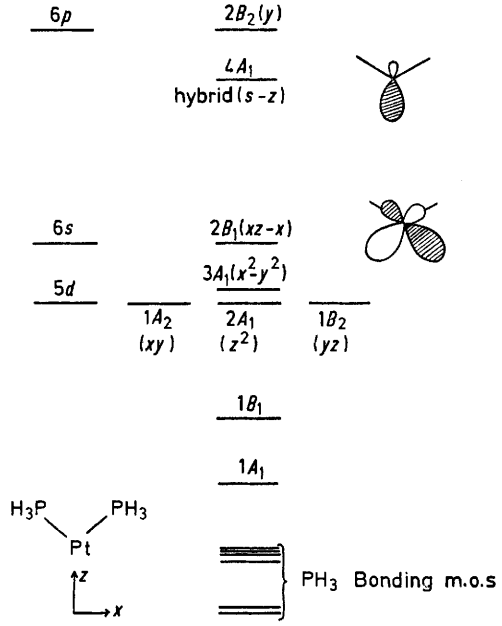

FIGURE 1 Calculated m.o.s for the $Pt(PH_3)_2$ fragment with P–Pt–P = 100°

Consider the simplified interaction diagram for an angular ML_2 fragment shown in Figure 2. In the formal scheme of setting up the interaction between the metal *xz* and *x* orbitals and the antisymmetric combination of ligand orbitals the metal–ligand mixing takes place to first order and gives rise to the bonding metal-phosphine molecular orbitals shown in Figure 1. However, the mixing of metal orbitals occurs as a second-order effect and the sign of mixing of *x* into *xz* is determined by the matrix element (2) where $L = 1/2^{\frac{1}{2}}(\phi_1 - \phi_2)$, *i.e.* the

$$\frac{\langle xz|L\rangle\langle L|x\rangle}{(E_{xz}-L)\,(E_{xz}-E_x)} \qquad (2)$$

antisymmetric combination of phosphine lone-pair orbitals.

If the interaction overlaps are chosen to be positive, as they are shown in Figure 2, then the numerator in (2) is positive. The sign of equation (2) is determined by the energy denominator. From the level ordering $E_L <$

* Throughout this paper the abbreviations *s*, *x*, *y*, *z*, *xz*, *yz*, z^2, $x^2 - y^2$, and *xy* are used for the corresponding metal *ns*, *np*, and $(n-1)d$ orbitals.

[22] F. A. Cotton and C. B. Harris, *Inorg. Chem.*, 1967, **6**, 369.
[23] L. Manojlovic-Muir, K. W. Muir, and J. A. Ibers, *Discuss. Faraday Soc.*, 1969, **47**, 84.
[24] F. R. Hartley, *Chem. Rev.*, 1969, **69**, 799.
[25] J. K. Burdett, *J.C.S. Faraday II*, 1974, 1549.

$E_{xz} < E_x$ the sign of equation (2) is negative for the donor orbital of the ML_2 fragment and therefore x (with the

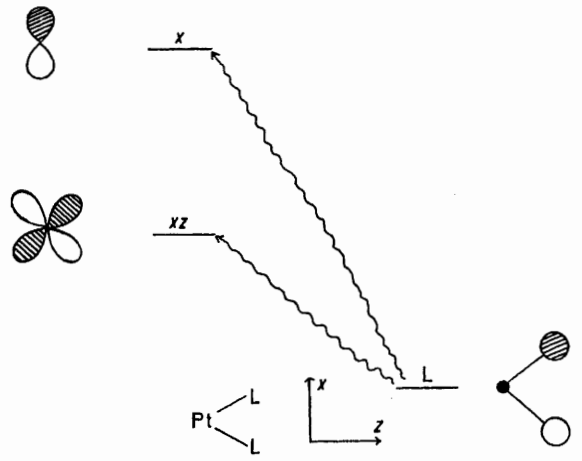

FIGURE 2 Simplified interaction diagram for the B_1 orbitals of the angular ML_2 fragment

phase defined in the Figure) mixes into d_{xz} with a minus sign. The result is therefore hybridisation away from the ligands in the manner shown below:

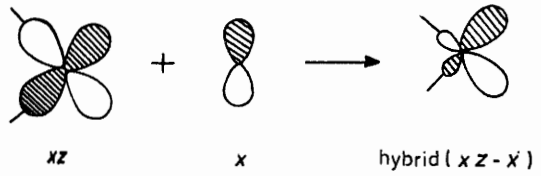

The platinum yz orbital does not rehybridise in the same fashion because its overlap with the ligand lone-pair symmetric and antisymmetric combinations is zero. A similar interaction diagram can be constructed for the symmetric combination of phosphine lone-pair orbitals and so accounts for the sign of mixing of the metal s and z orbitals in the lowest-unoccupied orbital (l.u.m.o.) of the $Pt(PH_3)_2$ fragment, *i.e.* hybrid(s–z) in Figure 1. At higher energies than hybrid(s–z) is the platinum $6p_y$ orbital.

The bonding capabilities of the $Pt(PH_3)_2$ are set primarily by the h.o.m.o. and l.u.m.o. The l.u.m.o. is ideally hybridised to accept an electron pair from a suitable donor orbital of an incoming ligand and the h.o.m.o. can provide effective back donation, in the P–Pt–P plane, to an empty orbital of b_1 symmetry on the ligand. The $Pt(PH_3)_2$ fragment is a poorer π donor in the plane perpendicular to P–Pt–P because the platinum y and yz orbitals are not hybridised effectively.

It is the superior back-donating capabilities of the platinum hybrid(xz) orbital which decides the conformations of platinum olefin, dioxygen, and di-imide complexes of the type $[PtL(PR_3)_2]$.[24] The bonding in such d^{10} complexes has been discussed in some detail by Rösch and Hoffmann [26] and by Cussachs and his co-workers.[27-29] It is my belief that the unequal bonding capabilities of the d_π orbitals of the $Pt(PH_3)_2$ fragment also decide the conformations of the carbaplatinaboranes (1) and (2).

(*b*) nido-*Icosahedral Fragment*.—The *nido*-$B_{11}H_{11}$ fragment (3) is derived from the parent icosahedron by the removal of a single vertex. It belongs to the C_{5v} point group and therefore the 11 boron atoms fall into three symmetry-inequivalent classes corresponding to those on the open pentagonal face, the closed pentagonal face, and finally the capping atom. Extended-Hückel calculations on this fragment have confirmed that it has

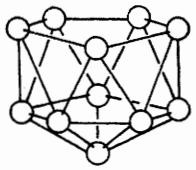

(3)

24 bonding m.o.s in agreement with simple electron-counting rules.[5] The higher lying of these m.o.s and the lowest-lying antibonding m.o.s are illustrated in Figure 3. In this Figure, for reasons of clarity, only those parts

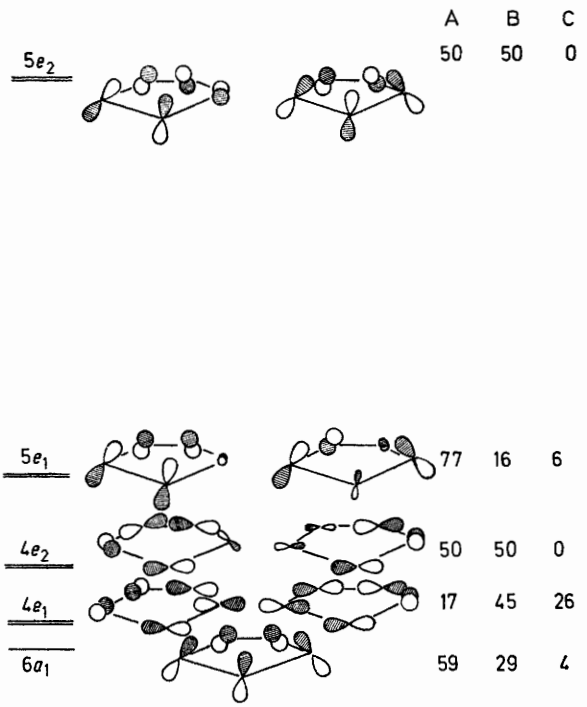

FIGURE 3 Frontier m.o.s of the *nido*-$B_{11}H_{11}$ fragment based on extended-Hückel calculations. The distribution of the m.o.s among the boron atoms on the open (A) and closed pentagonal (B) faces and the capping atom (C) is indicated on the right-hand side

of the m.o. wavefunctions which can be attributed to the open pentagonal face are shown. The relative contributions of the three symmetry-inequivalent classes of boron atoms to the total wavefunction are indicated at the right-hand side of the Figure.

The most interesting m.o.s from the point of view of

[26] N. Rösch and R. Hoffmann, *Inorg. Chem.*, 1974, **13**, 2656.
[27] J. H. Nelson, K. S. Wheelock, L. C. Cussachs, and H. B. Jonassen, *J. Amer. Chem. Soc.*, 1969, **91**, 7005.
[28] J. H. Nelson, K. S. Wheelock, L. C. Cussachs, and H. B. Jonassen, *Inorg. Chem.*, 1972, **11**, 422.
[29] K. S. Wheelock, J. M. Nelson, L. C. Cussachs, and H. B. Jonassen, *J. Amer. Chem. Soc.*, 1970, **92**, 5110.

the present analysis are those which are localised predominantly on the open face and are pointing out with respect to this face. The $6a_1$, $5e_1$, and $5e_2$ m.o.s. have these properties (see Figure 3) and furthermore bear a striking resemblance to the π m.o.s of the cyclopentadienyl anion. This conclusion is of course not unique, and indeed it formed the theoretical basis for Hawthorne's [30,31] original synthesis of 'dicarbollide' sandwich compounds. In contrast to the cyclopentadienyl anion the p_π orbitals of the $6a_1$, $5e_1$, and $5e_2$ m.o.s. of $B_{11}H_{11}$ are not orthogonal to the open pentagonal face but are rehybridised in such a way that they tilt inwards. This rehybridisation effect arises primarily because the hydrogen atoms attached to the boron atoms which define the open pentagonal face do not lie within that plane but above it. A similar rehybridisation phenomenon has been noted previously for co-ordinated carbocyclic ligands and has been discussed in detail elsewhere.[11]

For the $B_{11}H_{11}$ fragment there are four additional m.o.s ($4e_1$ and $4e_2$) which lie between the $5e_1$ and $6a_1$ orbitals in energy (see Figure 3). These orbitals, however, have their maximum amplitudes within the open pentagonal face of the *nido*-polyhedron and will overlap less effectively with the frontier orbitals of a metal fragment situated above this face. The role of the lower-lying $4e_1$-orbital set will be particularly small because it is localised predominantly on the closed pentagonal face and the capping atom rather than on the open face.

The carbaplatinaborane compounds shown in (1) and (2) can be constructed from a neutral $Pt(PR_3)_2$ fragment and the carbaboranes $B_9C_2H_{11}$ and $[B_{10}CH_{11}]^-$. The isoelectronic symmetric platinaborane $[B_{11}\{Pt(PH_3)_2\}H_{11}]^{2-}$ is derived from the $[B_{11}H_{11}]^{2-}$ anion and it is therefore necessary to introduce 46 electrons into the energy-level scheme for this anion. This results in an open-shell configuration . . . $(4e_2)^4(5e_1)^2$.

(*c*) *The Platinaborane Icosahedral Cluster*, $[B_{11}\{Pt(PH_3)_2\}H_{11}]^{2-}$.—Having analysed the characteristics of the frontier orbitals of the metal and icosahedral fragments, we are now in a position to evaluate the effect of bringing the fragments together to generate the hypothetical icosahedral cage molecule $[B_{11}\{Pt(PH_3)_2\}H_{11}]^{2-}$. The effect of carbon substitution into the open pentagonal face of the borane will then be considered as a perturbation of this scheme.

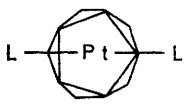

(4)

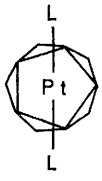

(5)

In $[B_{11}\{Pt(PH_3)_2\}H_{11}]^{2-}$ the angular metal-phosphine fragment can take up the two energetically equivalent conformations (4) and (5), each of which has C_s symmetry. Figure 4 illustrates schematically how the metal and *nido*-icosahedral fragments interact to generate the m.o.s of the platinaborane with the conformation (4). As is the case with cyclopentadienylmetal complexes,

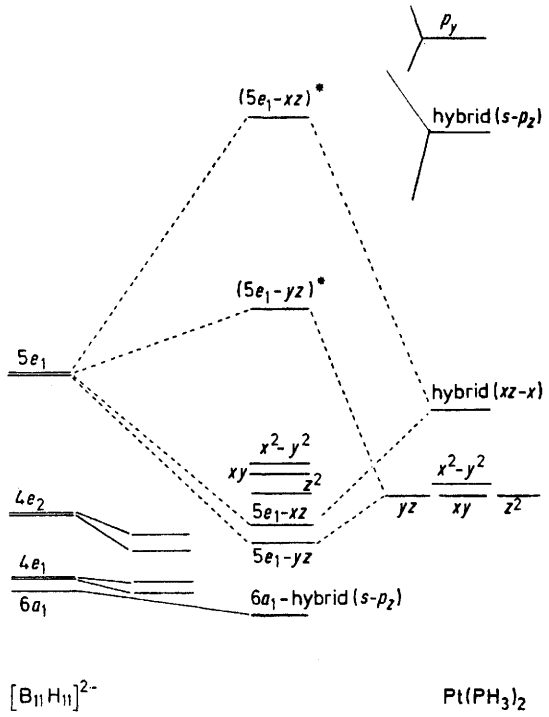

FIGURE 4 Interaction m.o. diagram for the union of the fragments $Pt(PH_3)_2$ and $[B_{11}H_{11}]^{2-}$. The platinaborane compound thus formed has the conformation (4)

the strongest metal–ligand interaction arises from the overlap of the out-pointing ligand orbitals of e_1 symmetry and the metal xz and yz orbitals.[32] For reasons which have been discussed in (*a*) above, the hybrid (xz) out-pointing d–p hybrid (6) overlaps more effectively with $5e_1$ (x) component (7) than the metal yz (8) with $5e_1$ (y) (9).

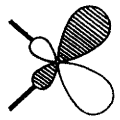

hybrid (xz-x)

(6)

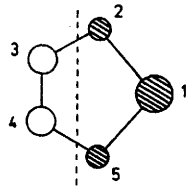

$5e_1$ (x)

(7)

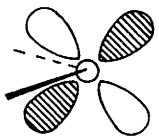

yz

(8)

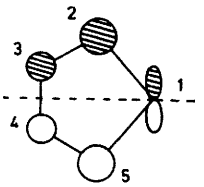

$5e_1$ (y)

(9)

[30] M. F. Hawthorne, 'The Chemistry of Boron and its Compounds,' ed. E. L. Muetterties, Wiley, New York, 1967.

[31] M. F. Hawthorne, D. C. Young, T. D. Andrews, D. V. Howe, R. L. Pilling, A. D. Pitts, M. Reintjes, L. F. Warren, and P. A. Wegner, *J. Amer. Chem. Soc.*, 1968, **90**, 879.

[32] For a recent summary of theoretical studies on η-cyclopentadienyl metal sandwich complexes see N. Rösch and K. H. Johnson, *Chem. Phys. Letters*, 1974, **24**, 179.

This distinction is enhanced by the more favourable energy match for the $5e_1(x)$–hybrid(xz) interacting pair (see Figure 4). A consequence of the relatively weak $5e_1(y)$–yz interaction is the low-lying antibonding orbital $5e_1(y)$–yz^* shown in Figure 4. The antibonding character of this orbital is somewhat mitigated by a mixing in of metal y character which hybridises the orbital way from the open face of the $[B_{11}H_{11}]^{2-}$ moiety as shown in (10).

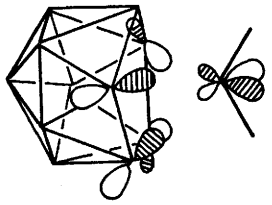

(10)

The metal $d_{x^2-y^2}$ and d_{xy} orbitals have δ pseudo-symmetry and enter into a weak antibonding interaction with the $4e_2$-orbital set of the ligand. This interaction is preferred to one with the higher-lying ' pseudo-cyclopentadienyl ' $5e_2$ orbitals. The z^2 orbital energy remains essentially unaffected, presumably because the p_π orbitals of the $6a_1$ ligand m.o. point towards the nodal cone of this orbital.[11] The $6a_1$ ligand orbital is stabilised by overlap with the empty, but high lying, sp hybrid of the $Pt(PH_3)_2$ fragment hybrid (s–z) in Figure 1.

For $[B_{11}\{Pt(PH_3)_2\}H_{11}]^{2-}$ the highest-occupied orbital is $5e_1(y)$–yz^* which as noted above is antibonding between the metal and ligand. The filled metal d_{yz} orbital therefore enters into a closed-shell four-electron destabilising interaction with the $5e_1(y)$ ligand orbital and the molecule owes its stability primarily to the hybrid(xz)–$e_1(x)$ two-electron bonding interaction.

It can be appreciated from the above analysis that the unequal bonding capabilities of the metal xz and yz orbitals play a major role in undermining the simple electron-counting rules. For the ML_2 fragment these rules suggest the presence of four non-bonding orbitals localised on the metal,[7] but the calculations on $[B_{11}\{Pt(PH_3)_2\}H_{11}]^{2-}$ indicate the presence of only three non-bonding orbitals and a low-lying antibonding orbital [$5e_1(y)$–yz^* in Figure 4]. The presence of an electron pair in this orbital gives rise to anisotropic metal–ligand antibonding effects which will be reflected in a range of platinum–boron bond lengths and lead to uncertainties about their classification as *nido* or *closo* structures. I will return to this point later, but first I discuss the electronic factors which could make the angular ML_2 fragment conform more closely to the electron-counting rules. The $5e_1(y)$–yz^* m.o. has some metal y character mixed into it in such a way that some of its antibonding character is reduced [see (10)]. A metal with a smaller d–p promotion energy than platinum [33] or stronger π-acceptor ligands than phosphines attached to the metal could reduce this antibonding character further. Therefore metallaboranes and carbaboranes based on $Ni(CO)_2$ and $Co(CO)(NO)$ fragments, for example, should give polyhedral geometries which are more closely related to those predicted on the basis of the polyhedral skeletal electron-pair theory.

The anisotropic bonding effects introduced by the filled $5e_1(y)$–yz^* orbital are seen in the calculated Mulliken overlap populations [34] for $[B_{11}\{Pt(PH_3)_2\}H_{11}]^{2-}$ which are given in (11a). The four-electron interaction [35,36] between yz and $5e_1(y)$ results in a higher electron population of the $5e_1(y)$ than the $5e_1(x)$ orbital and therefore the boron–boron overlap populations emphasise the nodal characteristics of the former [see (9)]. The platinum–boron overlap populations, in contrast, reflect the stronger bonding interaction between the metal hybrid(xz) orbital and the $5e_1(x)$ orbital. {For this orbital the magnitudes of boron $2p_\pi$-orbital coefficients follow the order $1 > 3,4 > 2,5$ [see (7)].}

For the other symmetrical conformation of the platinum complex [(5) above] a very similar interaction diagram can be constructed. The energy levels have the same energies but rotation of the $Pt(PH_3)_2$ fragment by 90°

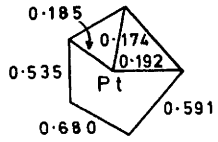

(11a)
[See (4)]

means that the metal hybrid(x) and yz orbitals interact with the complementary components of the $5e_1$ set, *i.e.* hybrid(xz) with $5e_1(y)$ and yz with $5e_1(x)$. Although the conformations (4) and (5) have equal energies, the calculated Mulliken-overlap populations for (5) follow a different pattern to that noted above for (4) [see (11b)]. For (5) the four-electron antibonding interaction occurs between $5e_1(x)$ and yz and therefore the boron–boron overlap populations in (11b) emphasise the nodal characteristics of the $5e_1(x)$ ligand m.o. [see (7)]. The

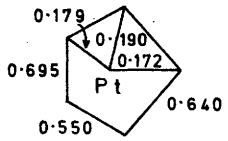

(11b)
[See (5)]

platinum hybrid(xz) orbital interacts exclusively with the ligand $5e_1(y)$ orbital in this conformation and the calculated platinum–boron overlap populations mirror the magnitudes of the boron $2p_\pi$ orbital coefficients in this orbital, *i.e.* $2,5 > 3,4 > 1$ [see (9)].

(*d*) *Carbaplatinaboranes.*—For $[B_{11}H_{11}]^{2-}$ the degeneracy of the $5e_1$ level leads to equal energies for the conformations (4) and (5), but when one moves on to consider the carbaboranes $[B_{10}CH_{11}]^{2-}$ and $B_9C_2H_{11}$ this degeneracy is removed and therefore the two extreme conformations need no longer be energetically equivalent. In-

[33] R. S. Nyholm, *Proc. Chem. Soc.*, 1961, 273.
[34] R. S. Mulliken, *J. Chem. Phys.*, 1955, **23**, 1833.
[35] L. Salem, *Proc. Roy. Soc.*, 1961, **A264**, 379.
[36] K. Muller, *Helv. Chim. Acta*, 1970, **53**, 1112.

deed the possibility of an intermediate and less symmetrical rotamer defined by the angle θ in (12) is also a distinct

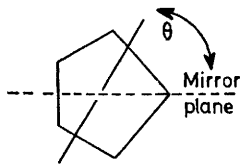

(12)

possibility. The symmetrical conformations [C_s symmetry shown in (13) and (14)] correspond to θ angles of 0 and 90° respectively. Extended-Hückel calculations

(13) (14)

on $[B_{10}C\{Pt(PH_3)_2\}H_{11}]^-$ for a range of angles from 0 to 90° have been completed and have been used to construct the Walsh diagram illustrated in Figure 5. From

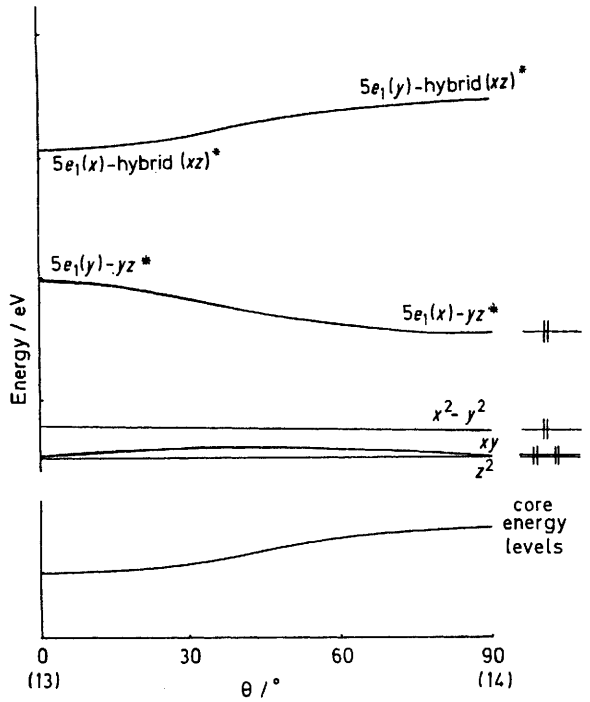

FIGURE 5 Walsh diagram for the rotation of the $Pt(PH_3)_2$ moiety in the compound $[B_{10}C\{Pt(PH_3)_2\}H_{11}]^-$. The extreme conformations (13) and (14) correspond to rotation angles (θ) of 0 and 90° respectively

this diagram it is clear that the highest-occupied m.o. is sensitive to changes in the angle θ and the total energy of the molecule reflects this sensitivity. Indeed the calculations indicate that the conformation (14) is the most stable and *ca.* 0.5 eV (48.25 kJ mol^{-1}) more stable than (13). The reason for the clear preference for the conformation (14) can be simply understood in terms of the following perturbation-theory analysis.[37-40]

The substitution of a single boron atom situated in the open pentagonal face of $[B_{11}H_{11}]^{2-}$ by carbon removes the degeneracy of the $5e_1$ level in the following manner: the

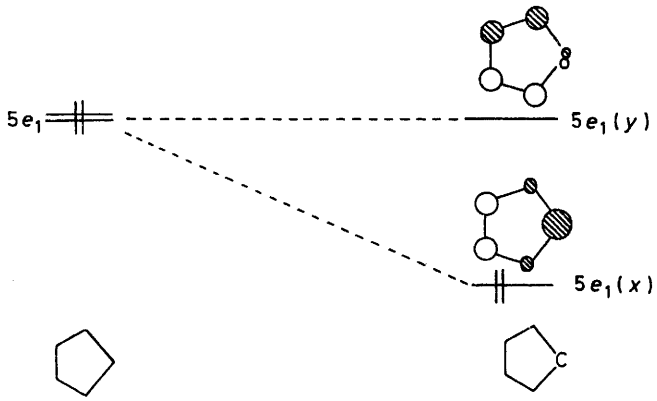

carbaborane $[B_{10}CH_{11}]^-$ anion has C_s symmetry and therefore the two components derived from $5e_1$ should strictly be labelled a'' and a'; however, as they retain the essential characteristics of the $5e_1$ level from which they were derived it is convenient to label them as $5e_1(x)$ and $5e_1(y)$. In $5e_1(y)$ the carbon atom lies along the nodal plane and therefore the energy of this component is essentially unaffected by the substitution. The $5e_1(x)$ component, in contrast, has a large contribution from the carbon $2p_\pi$ orbital and the lower-valence-state ionisation energy of this orbital compared to that of the boron $2p_\pi$ orbital results in a substantial stabilisation of this energy level (*ca.* 0.6 eV, 58 kJ mol^{-1}). Fuller details of the calculations relating to this substitution and a perturbation-theory analysis of the problem are given in the Appendix.

For the carbaplatinaborane compound, as in the parent ion $[B_{11}\{Pt(PH_3)_2\}H_{11}]^{2-}$, the major interfragment interactions arise from the $5e_1$ levels and the metal hybrid(*xz*) and *yz* orbitals. Figure 6 gives a schematic illustration of these important interactions for the two conformations (13) and (14). Only one of the metal hybrid(*xz*),*yz* orbital set can enter into a two-electron bonding interaction with one of the components of the $5e_1$ set; the other orbital must give rise to a four-electron antibonding interaction with the complementary $5e_1$ component. Clearly the most stable conformation will be that which gives rise to the most effective two-electron interaction and minimises the effects of the four-electron antibonding interaction. Figure 6 indicates that conformation (14) satisfies these requirements. The more favourable hybrid(*xz*)–$5e_1$ energy match in (14) gives a stronger bonding interaction and the antibonding *yz*–$5e_1$ orbital is less antibonding in this conformer [largely because $5e_1(x)$ is more stable than $5e_1(y)$].

The highest-occupied level has predominantly $5e_1(y)$

[37] R. Hoffmann, *Accounts Chem. Res.*, 1971, **4**, 1.
[38] L. Libit and R. Hoffmann, *J. Amer. Chem. Soc.*, 1974, **96**, 1370.
[39] W. L. Jørgenson and L. Salem, 'The Organic Chemists' Book of Orbitals,' Academic Press, New York, 1973.
[40] M. J. S. Dewar, 'The Molecular Orbital Theory of Organic Chemistry,' McGraw-Hill, New York, 1969.

character for (13) and $5e_1(x)$ for (14) and the lowest-unoccupied levels have complementary contributions from the $5e_1$ levels. Therefore, as the $Pt(PH_3)_2$ moiety is rotated to convert (13) into (14), the compositions of the highest-occupied and the lowest-unoccupied m.o.s must be smoothly reversed. As both m.o.s have the same symmetry characteristics when $\theta > 0$ but $<90°$, then this must be achieved by an 'avoided crossing'. The Walsh diagram in Figure 5 shows the characteristic features of such a strongly avoided level crossing.

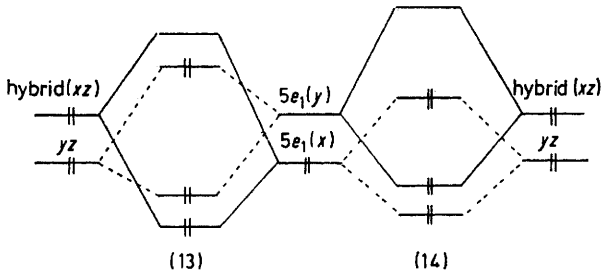

FIGURE 6 Schematic interaction diagrams for the two conformers (13) and (14) of $[B_{10}C\{Pt(PH_3)_2\}H_{11}]^-$

The above analysis is in excellent agreement with the *X*-ray studies of Welch and his co-workers who showed that the zwitterionic species (2) has the predicted conformation (14). Furthermore n.m.r. studies on this and related compounds indicate that the activation-energy barrier for rotation of the ML_2 moiety is large (>50 kJ mol^{-1}; calc. 36). The pseudo-isoelectronic compound B_8C_2[7][Pt(η-C_5H_5)[1]][Co(PEt_3)$_2$[8]]H_{10} which has a B_4C pentagonal face bonded to the platinum atom also has this conformation.

As with $[B_{11}\{Pt(PH_3)_2\}H_{11}]^{2-}$, the unequal bonding capabilities of the metal hybrid(*xz*) and *yz* orbitals result in a wide range of platinum–boron and boron–boron overlap populations. The calculated Mulliken-overlap populations for conformation (14) are shown in (15) and may

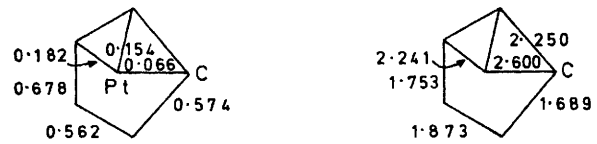

(15)

be contrasted with the experimentally determined bond lengths for (2).[15] The calculated overlap populations reproduce well the trends in B–B and Pd–B bond lengths and account nicely for the rather long Pd–C bond found in the *X*-ray crystallographic analysis. The small calculated Pd–C overlap population arises directly from the nodal characteristics of the $5e_1(y)$ orbital which provides the primary bonding interaction with hybrid(*xz*) [see (9)]. The B–C bond length cannot be compared directly with the B–B bond lengths and a correction which reflects the different covalent radii of these elements could perhaps be made to bring this bond length into line with the calculated overlap population.

In $B_9C_2H_{11}$ the degeneracy of the $5e_1$ level is also removed and the splitting is *ca.* 1 eV (96.5 kJ mol^{-1}). However, the sense of splitting is opposite to that noted above for $[B_{10}CH_{11}]^-$, *i.e.* $5e_1(y)$ lies at lower energies than $5e_1(x)$. This effect is illustrated schematically below and discussed in detail in the Appendix.

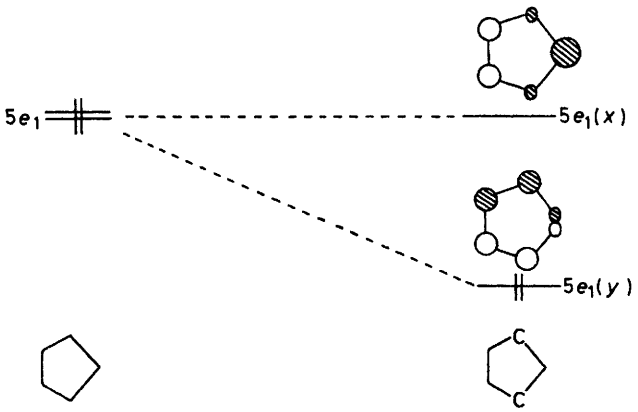

The carbaplatinaborane $B_9C_2[Pt(PH_3)_2]H_{11}$ also has two extreme conformations of C_s symmetry which are also defined by the rotation angle θ from the mirror plane. These rotamers are shown in (16) and (17). Therefore,

θ = 0 (16) θ = 90° (17)

as a direct result of the inversion of the $5e_1(x)$ and $5e_1(y)$ levels noted above, conformation (16) will be preferred for this compound. The relevant interaction diagrams for (16) and (17) are illustrated in Figure 7. Conformation (16) gives the more favourable hybrid(*xz*)–$5e_1$ h.o.m.o.–l.u.m.o. interaction and the antibonding $5e_1(y)$–*yz** orbital is lower lying for this conformation. This analysis is supported by the Walsh diagram for the rotation (Figure 8) based on extended-Hückel calculations on this compound. My calculations suggest that (16) is more stable than (17) by 57 kJ mol^{-1}. The energy barrier for the dicarbaborane is larger than that for the carbaborane discussed above because of the larger $5e_1(x)$–$5e_1(y)$ splitting in the former. *X*-Ray crystallographic

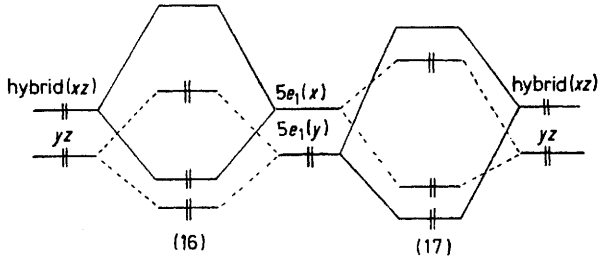

FIGURE 7 Schematic interaction diagram for the conformers (16) and (17) of $B_9C_2[Pt(PH_3)_2]H_{11}$

studies by Welch [14] on (1) have demonstrated that the conformation of this molecule closely approximates to that suggested by my calculations. The observed θ

angle is 10° and Welch [14] has suggested that this slight twist may arise from unfavourable intramolecular contacts for the symmetrical geometry.

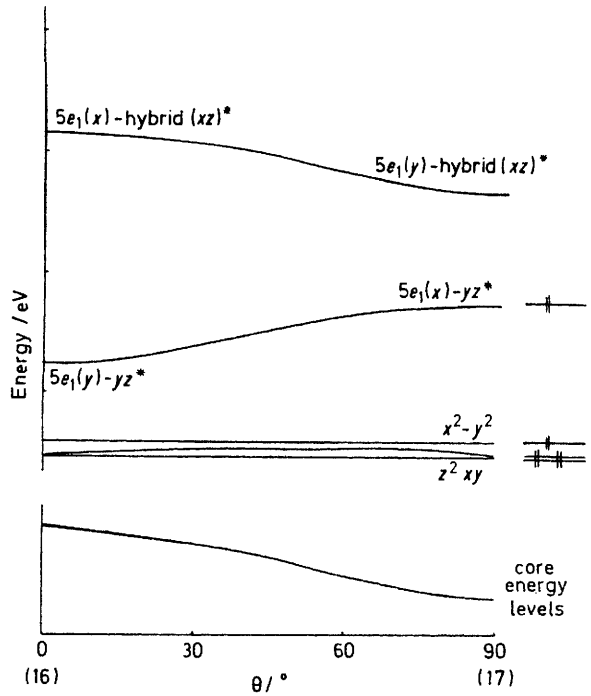

FIGURE 8 Walsh diagram for $B_9C_2[Pt(PH_3)_2]H_{11}$

The calculated overlap populations for this conformation once again reflect the unequal bonding effects of the metal hybrid(xz) and yz orbitals. The introduction of two carbon atoms into the open pentagonal face of $[B_{11}H_{11}]^{2-}$ leads to an exaggeration of the trends noted previously for $[B_{11}\{Pt(PH_3)_2\}H_{11}]^{2-}$ [see (11)]. In particular the platinum–carbon overlap populations are calculated to be rather small and reflect the predominant hybrid(xz)–$5e_1(x)$ bonding interaction for this conformer. The calculated overlap populations for the model compound and the observed bond lengths in (1) are compared

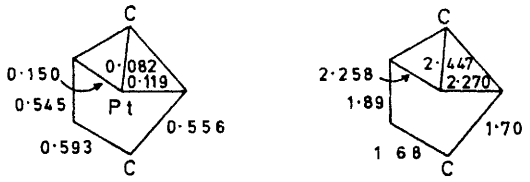

(1 8)

in (18). The overlap populations predict the correct trends for the Pt–C, Pt–B, and B–C bonds, but without making some arbitrary correction for differences in the covalent radii of boron and carbon it is not possible to draw any conclusions about the relative bond lengths for B–B and B–C bonds.

From the analysis above it is clear that the l.u.m.o. of the carbaborane icosahedral fragment and the h.o.m.o. of the platinum-phosphine fragment, hybrid(xz), decide the conformations of the carbaplatinaborane compounds. The preferred conformation is always that which gives the best overlap between hybrid(xz) and the l.u.m.o. of the carbaborane, *i.e.* $5e_1(y)$ for $[B_{10}CH_{11}]^-$ and $5e_1(x)$ for $B_9C_2H_{11}$. This suggestion could be profitably tested by more crystallographic studies on isomers of $B_9C_2H_{11}$ or more highly substituted derivatives, where the symmetry characteristics of the ligand l.u.m.o. could be easily established approximately by the perturbation-theory analysis given in the Appendix or by explicit m.o. calculations.

The m.o. calculations on carbaplatinaboranes discussed above also suggest that d^8 metal bis(phosphine) compounds of these carbaboranes are a distinct possibility. Indeed, compounds such as $B_9C_2[Os(PR_3)_2]H_{11}$ may prove to be thermodynamically more stable than the corresponding platinum compounds because they would avoid the four-electron destabilising interaction between $5e_1$ and yz (see Figures 5 and 8). The other interesting conclusion which can be reached about such compounds is that their conformations will be complementary to those discussed above for platinum. Examination of the Walsh diagrams in Figures 5 and 8 suggest that removal of an electron pair from the h.o.m.o. will remove the driving force which stabilises the conformers (14) and (16), and the conformers (13) and (17) are favoured by the energy–θ characteristics of the core levels. The reason for this preference can be appreciated from the following simplified interaction diagram for a $B_9C_2H_{11}$ d^8 compound:

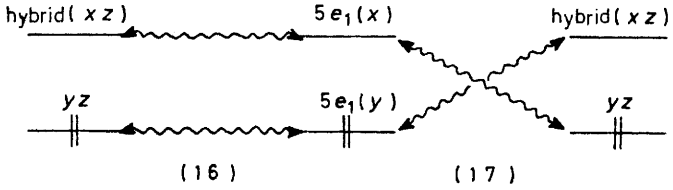

Conformation (17) allows two effective h.o.m.o.–l.u.m.o. charge-transfer interactions, whereas (16) generates an unfavourable four-electron antibonding interaction and therefore (17) will be the more stable.

APPENDIX

Perturbation-theory Analysis of the Effect of Carbon Substitution in the Pentagonal B_5H_5 *Ring.*—The p_π orbitals of a planar B_5 ring, ϕ_i, give rise to a degenerate set of m.o.s of e_1 symmetry with the eigenvectors and eigenvalues within the Hückel approximation in equations (A1)—(A3).

$$\psi_1^\circ[e_1(y)] = (2/5)^{\frac{1}{2}}(\sin 72^\circ\phi_2 + \sin 36^\circ\phi_3 - \sin 36^\circ\phi_4 - \sin 72^\circ\phi_5) \quad \text{(A1)}$$

$$\psi_1^\circ[e_1(x)] = (2/5)^{\frac{1}{2}}(\cos 72^\circ\phi_2 - \cos 36^\circ\phi_3 - \cos 36^\circ\phi_4 + \cos 72^\circ\phi_5 + \phi_1) \quad \text{(A2)}$$

$$E^\circ[e_1(x)] = E^\circ[e_1(y)] = \alpha + 0.618\beta \quad \text{(A3)}$$

The labels x and y refer to the location of the nodal planes [see (7) and (9) above]. To first order in ε a perturbation εH^1 will give rise to new energy levels with energies given by (A4) [37–40] where E_k^1 are the eigenvalues of the

$$E = E^\circ + \varepsilon E_k^1 \ (k = 1 \text{ or } 2) \quad \text{(A4)}$$

matrix D and $d_{jk} = (\psi_j^\circ)^T H^1(\psi_k^\circ) = d_{kj}$. If $(p_{k1}\, p_{k2}, \ldots p_{kn})$

$$D = \begin{vmatrix} d_{11} - E^1 & d_{12} \\ d_{21} & d_{22} - E^1 \end{vmatrix} = 0$$

is an eigenvector of D with eigenvalue E_k^1 then the zero-order eigenvector of H (where $H = H^\circ + \varepsilon H^1$) corresponding to the energy level (A4) is (A5). If the boron atom B_n

$$\psi_k = p_{k1}\psi_1^\circ + p_{k2}\psi_2^\circ \qquad \text{(A5)}$$

(n = 1—5) is replaced by carbon which is more electronegative the perturbation can be modelled by setting the appropriate Coulomb integral $\alpha_n = \alpha + (\beta/2)$. In the expressions given above, $\varepsilon = \frac{1}{2}$ and the diagonal element of the perturbing Hamiltonian, H^1, is $H_{nn}^1 = \beta$.

The analysis is simplified considerably if the carbon atom is chosen to lie on the nodal plane of ψ_1° [$e_1(y)$] above, *i.e.* substitution at the 1 position. If this is done the off-diagonal elements of the matrix D, d_{12} and d_{21}, are zero and therefore the original wavefunctions ψ_1° and ψ_2° retain their essential characteristics. Furthermore, the first-order perturbation energy depends only on the square of the coefficients of the p orbital at the position of substitution. Therefore $E_1^1 = 0$ and $E_2^1 = \varepsilon . \frac{2}{5} . 1^2 . \beta = \beta/5$, *i.e.* the energy of ψ_1° [e_1 (y)] is unchanged and ψ_1°[e_1 (x)] is stabilised by $\beta/5$.

For the disubstituted carbaborane ring (B_3C_2), if the carbon atoms are symmetrically situated with respect to the nodal plane of ψ_1° (*i.e.* positions 2 and 5), the D matrix also simplifies in the sense that $d_{12} = d_{21} = 0$ and the first-order perturbation theory energies are: $E_1^1 = \varepsilon[(2/5)\sin^2 72 + (2/5)\sin^2 72]\beta = 0.362\beta$; $E_2^1 = \varepsilon[(2/5)\cos^2 72 + (2/5)\cos^2 72]\beta + 0.076\beta$. Thus both $\psi_1^\circ[e_1(y)]$ and $\psi_1^\circ[e_1(x)]$ are stabilised but the former by a greater amount. The results of this perturbation-theory analysis are presented in a diagrammatic form below:

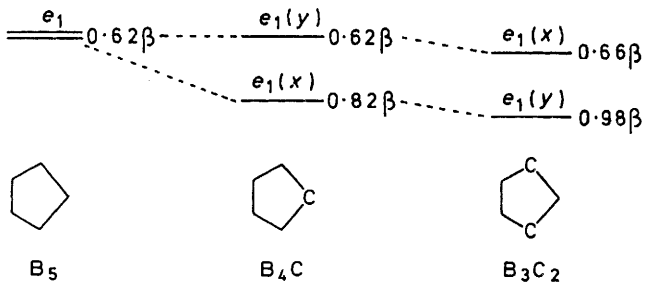

The above analysis was confirmed by extended-Hückel calculations on $[B_{11}H_{11}]^{2-}$, $[B_{10}CH_{11}]^-$, and $B_9C_2H_{11}$. The relevant eigenvalues (eV) are given below:

	$[B_{11}H_{11}]^{2-}$	$[B_{10}CH_{11}]^-$	$B_9C_2H_{11}$
$5e_1(y)$	−9.4912	−9.5573	−10.8125
$5e_1(x)$	−9.4912	−10.2128	−9.7882

The first-order perturbation-theory analysis given above suggests that the wavefunctions for $e_1(x)$ and $e_1(y)$ are unchanged. Higher-order perturbation theory which permits polarisation effects will remove this characteristic, but as the analysis does not depend on the precise values of the coefficients but rather on the nodal characteristics of the orbitals I will not discuss this point in detail in this paper.

[6/1036 *Received, 2nd June,* 1976]